Optical Measurement of Transverse Molecular Diffusion in a Microchannel

Andrew Evan Kamholz, Eric A. Schilling, and Paul Yager
Department of Bioengineering, University of Washington, Seattle, Washington 98195 USA

ABSTRACT Quantitative analysis of molecular diffusion is a necessity for the efficient design of most microfluidic devices as well as an important biophysical method in its own right. This study demonstrates the rapid measurement of diffusion coefficients of large and small molecules in a microfluidic device, the T-sensor, by means of conventional epifluorescence microscopy. Data were collected by monitoring the transverse flux of analyte from a sample stream into a second stream flowing alongside it. As indicated by the low Reynolds numbers of the system (<1), flow is laminar, and molecular transport between streams occurs only by diffusion. Quantitative determinations were made by fitting data with predictions of a one-dimensional model. Analysis was made of the flow development and its effect on the distribution of diffusing analyte using a three-dimensional modeling software package. Diffusion coefficients were measured for four fluorescently labeled molecules: fluorescein-biotin, insulin, ovalbumin, and streptavidin. The resulting values differed from accepted results by an average of 2.4%. Microfluidic system parameters can be selected to achieve accurate diffusion coefficient measurements and to optimize other microfluidic devices that rely on precise transverse transport of molecules.

INTRODUCTION

Diffusion of analytes is often critical to the operation, accuracy, and efficiency of microfluidic devices for DNA analysis (Chen and Chen, 2000; Ehrlich and Matsudaira, 1999; Khandurina et al., 2000), mass spectrometry (Chan et al., 1999; Li et al., 2000; Pinto et al., 2000), biosensors (Kamholz et al., 1999; Macounova et al., 2000; Yang et al., 2000), surface patterning (Bernard et al., 1998; Chiu et al., 2000; Folch and Toner, 1998; Kenis et al., 1999), and other applications. This study demonstrates quantitative measurement of analyte diffusivity by observing spatial distributions across a microchannel. The applications of this work include aiding in the design of microfluidic devices based on desirable distributions of diffusing analyte and the analysis of data collected from such devices.

The T-sensor is a microfluidic device in which analyte diffusion is exploited to make diagnostic determinations of analyte concentrations (Weigl and Yager, 1999). In its simplest configuration, the T-sensor introduces two fluid streams side by side (Fig. 1). One stream contains the analyte of interest; the other stream contains a receptor molecule, which could be an antibody (Hatch, A., A. E. Kamholz, B. H. Weigl, and P. Yager, manuscript submitted), pH indicator (Galambos et al., 1997), fluorescent indicator (Kamholz et al., 1999), or other reactive species. The interdiffusion of molecules from the two input streams induces a measurable signal, usually optical, that can be correlated with a parameter of interest (i.e., analyte concentration, diffusion coefficient, binding affinity). This correlation can be made empirically by comparing the measured signal with a calibration curve, or analytically by fitting the measured data to results from numerical simulations that include all relevant parameters.

Fluid actuation in the T-sensor has typically been achieved through pressure-driven flow (via positive displacement pumping) because of the low cost, flexibility, and insensitivity to sample and surface characteristics. The device cross-section has one long dimension, the diffusion dimension d, and one short dimension, the width w. If the aspect ratio d/w is greater than about 4, the fully developed velocity profile will be parabolic across w and approximately blunt across d (Happel and Brenner, 1973). The devices used in this study ranged in aspect ratio from 180 to 240. The development of flow velocity along the length of a typical T-sensor is shown in Fig. 2. The z-velocity at the stagnation point, the point where the two inlet channels meet, is zero but increases rapidly until flow is fully developed.

In practice, the optical signal most commonly detected in the T-sensor is fluorescence emission. Such detection can be accomplished conveniently with conventional epifluorescence microscopy. Collection of the optical signal as in Fig. 1, however, integrates through the narrow dimension of the T-sensor, the width w. A previous study characterized the non-uniformity of diffusing analyte across w induced by the velocity gradient and the effect of this phenomenon on measurements in the T-sensor (Kamholz and Yager, 2001). Such artifacts were attenuated in devices with narrower w-dimensions.

This study presents a rapid method for measurement of the diffusion coefficient for molecular species that span the size range of interest for biochemistry. Examples include fluorescently labeled biotin and three proteins of varying molecular weight. Also included are considerations of how

Received for publication 15 September 2000 and in final form 13 December 2000.

Address reprint requests to Paul Yager, Department of Bioengineering, Box 352255, University of Washington, Seattle, WA 98195. Tel.: 206-543-6126; Fax: 206-543-6124; E-mail: yagerp@u.washington.edu.

0006-3495/01/04/1967/06 $2.00

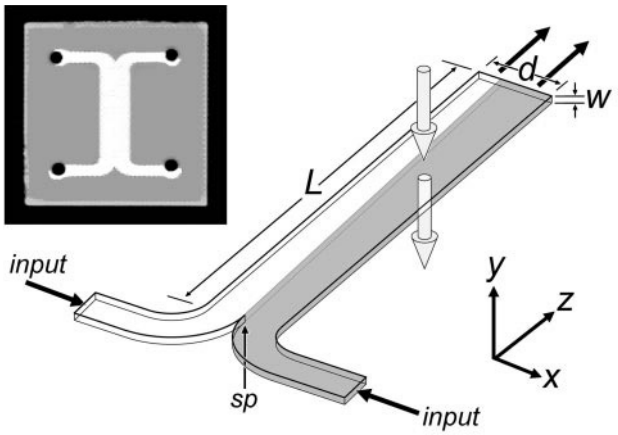

FIGURE 1 (*Top left*) Optical micrograph of a T-sensor used in this study. The device has two input ports and two output ports, although the split output is not necessary for this study. For scale, the circular access ports are 1 mm in diameter and the entire chip is 15 mm square. (*Bottom right*) Conceptual rendering of the operation of the T-sensor. Two fluid inputs enter through channels at the bottom, merging at the stagnation point (sp). In the case shown here, the fluid on the right contains a diffusable analyte (gray) that spreads across the *d*-dimension as flow proceeds along the channel length. Measurements made in this study by fluorescence detection occur along the optical axis, denoted with *large arrows* in the *y*-direction.

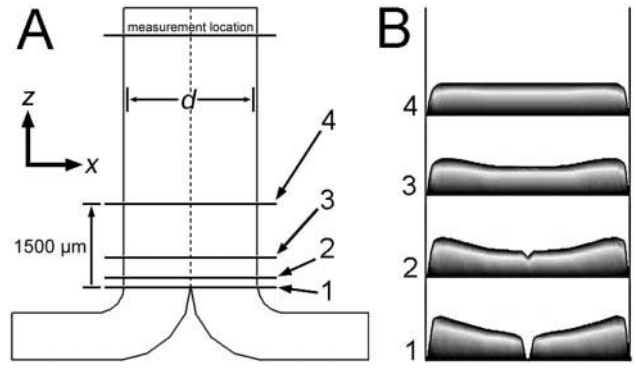

FIGURE 2 Three-dimensional finite element simulations of the velocity profile development in a typical T-sensor used in this study, measuring 2405 μm across the diffusion dimension (*d*) and 10 μm across the width (*w*, into page). For the four numbered locations marked in *A*, velocity profiles in the *y*-direction at the ½ *w* plane are shown in *B*. Over the flow rate range used in this study, the velocity profiles all have the same shape and relative magnitudes. The entry length along the channel midline was 864 μm to 95% of fully developed velocity and 1423 μm to 99%. In the actual experiments, all diffusion coefficient data were collected at 5000 μm downstream. The three-dimensional simulations were done using FlumeCAD. See the Experimental Section for more detail on this simulation package.

the details of device design and implementation of a specific optical detection system impact measured results.

EXPERIMENTAL SECTION

Device fabrication

Microfluidic devices were created using the facilities of the Washington Technology Center (Seattle, WA). Standard photolithographic techniques described elsewhere (Brody et al., 1997) were used to create channels in a test-grade 4-in silicon substrate (International Wafer Service, Portola Valley, CA). The wafer was oxidized in a furnace to form approximately 4000 Å of oxide. A negative photoresist (AZ1512, Clariant Corp., Somerville, NJ) was applied in a spin-coat, baked on a hot plate, and patterned by selective exposure to ultraviolet light. The mask consisted of a high-resolution transparency film printed to scale and mounted on a clear glass slide. After developing the photoresist, all exposed oxide was etched with a hydrofluoric acid etchant, and the exposed silicon was etched with KOH to a depth of 10 μm. Fluid access ports were drilled manually with a diamond-tipped bit (TSI Inc., Seattle, WA) using a rotary tool (Dremel, Racine, WI). The channels were enclosed by a borosilicate wafer (U.S. Precision Glass, Elgin, IL) anodically bonded to the silicon. The wafer was diced to produce 16 separate devices.

Fluid handling

The two input fluids were delivered to the T-sensor using computer-controlled syringe pumps (Kloehn Co. Ltd., Las Vegas, NV). The syringe size ranged from 25 to 100 μl, depending on which was most convenient for delivering a particular flow rate in the range studied. All fluid lines and fittings were made from rigid polyetheretherketone (PEEK; Upchurch Scientific, Oak Harbor, WA). A custom-built aluminum manifold that has been previously described (Kamholz et al., 1999) was used to bring fluid lines in contact with access ports on the silicon face of the device. The syringe pumps could provide pressures much greater than those produced by the resistance of the channels. Pumps were controlled via a simple communication protocol from an attached PC.

Optical detection and image capture

The diffusion of the analyte molecules studied was monitored by the fluorescence of the analytes themselves. Traditional epi-illumination fluorescence microscopy was used (IM35 inverted microscope; Zeiss, Thornwood, NY) with the device placed on the microscope stage with the glass side facing toward the objective. A 10× or 20× objective was used with a 100 W mercury arc source (Zeiss) providing excitation light. The intensity of excitation being delivered to the sample was measured using a power meter (Model 212, Coherent Inc., Auburn, CA) and found to be approximately 40 W/cm^2 through the 10× objective and fluorescein filter set. Using bright-field illumination, it was confirmed that the depth of focus was sufficient to bring the entire device into focus. Care was taken to focus at the middle of the channel (at ½*w*) so that fluorescence emission would be collected as evenly as possible throughout the *w*-dimension (Fig. 1). Slight changes (up to $\pm$10 μm) in the plane of focus did not substantially affect the measurements (<3%).

The fluorescence signal was collected with a color three-chip cooled CCD camera (ChromoCam 300, Oncor, Gaithersburg, MD). The linearity of the camera response to light intensity was checked by flooding the device with different concentrations of fluorophore. At the default camera settings, which include an automatic image-enhancement-algorithm (gamma), the response was best fit with a near-linear second order polynomial. As shown below in this study, accurate diffusion measurements at all flow rates were obtained only by including the nonlinear response function in the analysis of the images. Disabling the enhancement algorithm restored the linear relationship.

The choice of integration time for a particular experiment depended on the fluorescence intensity of the analyte being studied and ranged from 1 to 7 s. Acquisition of integrated frames was made with a frame-grabber card (CG-7; Scion Corp., Frederick, MD) mounted in a PC. Additional

frames were captured while the device was flooded with fluorophore to be used in correcting for the spatial non-uniformity of the mercury arc source and the illumination/collection optics and for calibrating the camera response.

Fluorescence intensity values across each image were extracted using a custom-coded MATLAB (The MathWorks Inc., Cambridge, MA) program. An average from 10 lines of pixels centered at 5000 μm downstream was used. The data were transferred in numerical form to Microsoft Excel for comparison with results from simulations. Some data sets were then transformed to concentration using the measured camera response function. The remaining sets were transformed assuming a linear relationship between signal intensity and concentration. Each data set was normalized so that the baseline value (no signal) was 0 and the signal from the bulk analyte was 1. Then, each data set was shifted horizontally so that the 0.5 intensity value coincided with the center of the channel at $\frac{1}{2}d$.

Diffusion coefficient measurements

For all measurements, a stock buffer of 100 mM Tris-HNO_3, pH 7.9, was used. Experiments were conducted over a large range of flow rates for fluorescein-biotin (B-8889, Sigma, St. Louis, MO). The flow rate range was limited at the low end (41.7 nl/s) by the slowest flow rate achievable with the 25 μl syringes. The maximum flow rate (1000 nl/s) was determined by the need to allow enough diffusion to occur to make precise measurements. Based on an average flow rate of 500 nl/s and an average image integration time of 4 s, the theoretical lower limit of required sample volume is 2 μl. Due to the axial dispersion generated by pressure-driven flow, however, the practical lower limit is 3 to 5 times this volume.

Devices and associated tubing were cleaned before all experimental trials by rinsing with several milliliters of 10% bleach followed by several milliliters of water. Four complete sets of measurements were conducted for fluorescein-biotin in order to study the effects of considering the camera response function and varying the illumination intensity. The first two sets illuminated a sample of 2.5 μM analyte using the full excitation intensity of the mercury arc source. In the first set, the nonlinear camera response was considered while in the second set it was neglected. The third set used excitation intensity reduced to 19% at 488 nm, whereas the fourth set used only 5% of the full intensity. In order to maintain adequate signal-to-noise ratios, the third and fourth sets used increased fluorescein-biotin concentrations of 16.7 and 50 μM, respectively. The camera response function was also ignored for the analysis of these last two sets. Attenuation of arc source intensity was achieved using combinations of neutral density filters. Based on the minimum practical sample size of 10 μl, the concentration range used in this study represents between 25 and 500 picomoles of analyte.

Several fluorescent-labeled proteins of interest were also tested at a limited number of flow rates within the range of interest. They were FITC insulin (10 μM, mono-labeled, zinc-free, I-13269, Molecular Probes, Eugene, OR), streptavidin Alexa Fluor 488 (1 μM, S-11223, Molecular Probes), and fluorescein-ovalbumin (1 μM, O-835, Molecular Probes). These proteins adsorbed to the surface of the devices as demonstrated by residual fluorescence signal in the channels after washing with buffer. Therefore, the devices used were pretreated with a 50 μM solution of unlabeled bovine serum albumin (A-7030, Sigma) in stock buffer. The device was filled with the bovine serum albumin solution, placed in a beaker of the same solution for 2 h, and dried under flowing N_2. Treated devices could be used for about an hour before the sample proteins began to noticeably displace the bovine serum albumin on the surface, increasing the background fluorescence.

For a typical T-sensor experiment, two input fluids were used. One stream contained the analyte of interest dissolved in stock buffer; the other stream contained only buffer. The concentrations of analytes were chosen such that the intensity of the fluorescence emission was bright enough to avoid integration longer than 8 s. All analytes were dilute enough to have a negligible effect on the viscosity (estimated $<0.1\%$) and to eliminate significant molecule-molecule interactions. All measurements were conducted at room temperature.

In a previous study (Kamholz and Yager, 2001), it was concluded that wider devices (larger w-dimension) produce artifacts when making measurements in the T-sensor due to the parabolic velocity profile across the width. The distribution in residence time among the fluid laminae affects the spatial distribution of diffusing analytes. The study found that using a width of 10 μm with fluorescein-biotin produced less than 5% error over the flow rate range used in the present study. Therefore, this value was used for w in this study; narrower devices are very difficult to load due to extremely high fluidic resistance. Recalling that the minimum flow rate was limited by the slowest step rate of the pumps, the only way to increase the average residence time to allow substantial transverse diffusion to occur was to increase d. The diffusion dimension of devices used in this study ranged from 1870 to 2400 μm. In the experiments with the slowest flow rate and most quickly-diffusing analyte, the entire interdiffusion zone encompassed less than 200 μm of the center of the channel. Therefore, any non-uniformity in the velocity profile at the extremes of the d-dimension was irrelevant to this study.

The maximum flow rate used in this study was 1 μl/s. The Reynolds number (Re) is given by:

$$\mathrm{Re}_w = \frac{\rho v_{av} w}{\mu} \tag{1}$$

where ρ is fluid density (taken as 1 g/cm^3), v_{av} is average fluid velocity, w is width (the most relevant length scale for this system), and μ is fluid viscosity (taken as 1 cP). The Reynolds number range used in this study was 0.02 to 0.41, indicating purely laminar flow.

After collecting data, diffusion coefficients were determined by finding the best fit between the experimental results and the predictions of a previously described one-dimensional numerical simulation (Kamholz et al., 1999). The best fit was achieved by finding the least residual between the experimental and predicted data sets.

Data analysis

Experimental data sets were analyzed by one of two methods. The first method assumed that the camera response was linear with fluorophore concentration (when, in fact, it had been automatically enhanced so that it was *not* linear). This method proved to be adequate at higher flow rates but substantially inaccurate at the slower flow rates tested. First, data images were divided by a flooded image in order to account for spatial non-uniformity of the excitation light and optical elements. This image was taken when the device was flooded with the same concentration of fluorophore used to run the experiments. Although the solution of an idealized one-dimensional diffusion problem yields a perfectly symmetric sigmoid (Crank, 1956), some of the diffusion curves collected by this method were asymmetric (see Results and Discussion and Fig. 3). All experimental data were well fit by sigmoids in the region where the analyte concentration was greater than half the starting concentration. However, the low concentration tails of some curves fell below the expected sigmoid curves. Therefore, only the top half of the non-sigmoidal curves (normalized intensity >0.5) were considered when fitting with the results of the one-dimensional model, which always produces a perfect sigmoid. The second method of data analysis included measurement of the actual camera response as a function of concentration, rather than assuming a linear relationship. The response was measured by flooding the channel with several different fluorophore concentrations and fitting the resulting intensity-versus-concentration curve with a second order polynomial. The polynomial coefficients were then used to transform the raw intensity data from experimental images to concentration values. Fitting of the polynomial function was done at each pixel across the image, thereby also accounting for non-uniformity in the excitation intensity. These data sets were fit accurately by sigmoidal curves and all data points for each trial were used for fitting (as

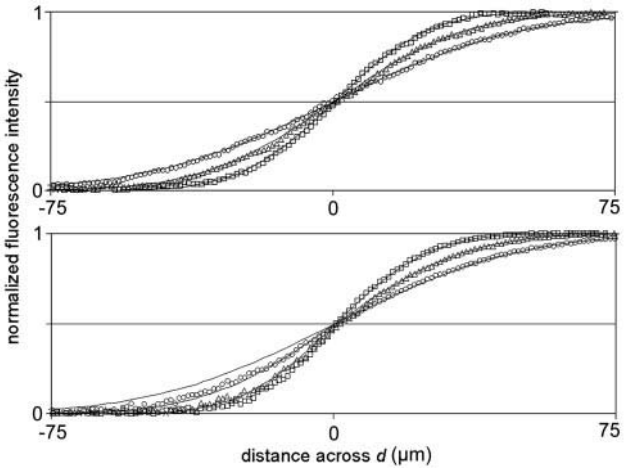

FIGURE 3 Comparison of experimental diffusion data over a range of flow rates for the small molecule fluorescein-biotin. Data points represent fluorescent intensity contours taken at 5000 μm downstream. Solid lines are numerical fits with the one-dimensional model. The top panel is for 2.5 μM fluorescein-biotin at full illumination intensity, analyzed after correcting for the camera response function. In the bottom panel, 50 μM of fluorescein-biotin was used, illumination intensity was reduced by 94% at 488 nm, and the camera response function was neglected. Data sets were first normalized and then shifted left to right so that the 0.5 intensity value occurred at a distance across d of 0. The curves in the top portion display sigmoid symmetry; those in the bottom panel do not. Data are not shown for two intermediate cases where the degree of symmetry was intermediate. For the asymmetric data sets, fits were made only to the upper half of each curve (intensity >0.5). For symmetric sets, fits were made to all points. Total input flow rates for both panels: ○ = 41.7 nl/s, △ = 83.3 nl/s, □ = 166.7 nl/s.

opposed to the case above, where only half the points were used). As this method did not necessitate partial fitting and yielded accurate results over the entire flow rate range, it is the preferred method for data analysis.

Quantification of entry effects using three-dimensional numerical simulations

A potential source of error in calculation of diffusion coefficients is the fact that the assumption of a fully developed velocity profile at all times is not correct. Rather, the velocity at the fluid interface at ½d accelerates to the final velocity from a stagnation point. To quantify the flow development, three-dimensional hydrodynamic and mass transport simulations were performed using the NetFlow module of FlumeCAD (Microcosm Technologies, Inc., Cary, NC) run on a Sun Microsystems (Palo Alto, CA) Ultra-10 workstation with 256 MB of RAM. A three-dimensional finite element mesh of the T-sensor geometry used in this study was drawn with the accompanying SDRC Ideas software (Milford, OH). Volumetric flow rate boundary conditions that spanned the range used in this study were specified in separate simulations at both inlets of the T-sensor. Values of the velocity field were recovered from the simulations in order to determine flow development entry lengths. Diffusion simulations took about 1 day to run and produced coarse solutions, limiting their efficacy for quantitative predictions of the operation of the T-sensor. However, the solutions were good enough to estimate the magnitude of effects produced by the flow-development region, particularly the development of the velocity in the center of the channel (at ½ d), which starts at 0 at the stagnation point (see Fig. 1 for stagnation point location). These simulations also produced the velocity profiles in Fig. 2.

RESULTS AND DISCUSSION

Diffusion coefficient measurements

Typical normalized data from the experiments with fluorescein-biotin are shown in Fig. 3. For the data set that was analyzed after taking into account the true camera response function (top of Fig. 3), the curves are sigmoidal and are well fit by the model predictions over the entire concentration range. For the data sets where the camera response function was ignored (bottom of Fig. 3), the curves have varying degrees of asymmetry, and many of the fits are poor below concentrations of 0.5.

Fig. 4 plots the dependence of the apparent diffusion coefficient on flow rate over the studied flow rate range for each of the four experimental sets. Based on the molecular weight of the fluorescein-biotin conjugate (831 D) and reported diffusion coefficients of molecules of similar mass (Perry, 1950), the diffusion coefficient of fluorescein-biotin should be approximately 3.4×10^{-6} cm^2/s. Among the four sets of experiments, only the data corrected for the nonlinear camera response produced accurate measurements of the diffusion coefficients over the entire flow rate range. The other three data sets show varying degrees of error and indicate a dependence on the intensity of excitation, with the largest errors occurring when the excitation intensity was the strongest. Although this initially suggested that photobleaching of the fluorescein might contribute to errors, further experiments precluded this possibility. Some of the experiments were repeated using a custom-built filter that blocked the excitation light from the T-sensor entrance until

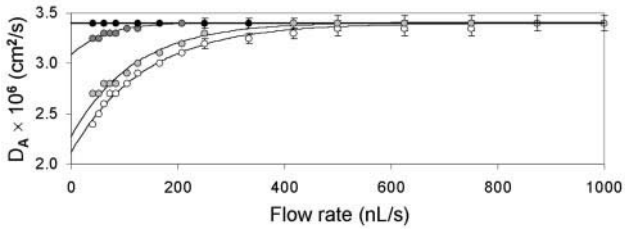

FIGURE 4 Measurements of the apparent diffusion coefficient of fluorescein-biotin over a range of flow rates. The heavy line represents the expected value of 3.4×10^{-6} cm^2/s. Values were obtained by fitting diffusion contours with the one-dimensional model (as in Fig. 3) and are summarized here over all flow rates tested. The *black circles* are for 2.5 μM fluorescein-biotin at full illumination intensity and analyzed with the camera response function. All other data sets were analyzed without using the camera response function (assuming a linear intensity-versus-concentration relationship): the *dark gray circles* are for 16.7 μM fluorescein biotin with excitation intensity at 488 nm reduced to 19%, the *light gray circles* are for 50 μM at excitation intensity reduced to 5%, and the *white circles* are for 2.5 μM at full excitation intensity. Only the measurements made when considering the camera response function (*black circles*) are accurate over the entire flow rate range, although all measurements are accurate above a flow rate of about 500 nl/s. Error bars, representing the precision used in model fits, are smaller than the symbol size where absent. The solid curves are shown only for clarity.

the point of measurement at 5000 μm downstream, reducing the exposure time of the fluorescein-biotin before measurement by at least a factor of 10. These results were indistinguishable from identical experiments without the blocking filter. Moreover, the time constant for fluorescein photobleaching was measured in the same T-sensor (under nonflowing conditions) at 91 s, but the average residence time varied from just 0.1 s to 2.9 s over the flow rate range. Therefore, it is concluded that no substantial photobleaching occurred during any of the experiments. The differing degrees of error, among those data sets for which the camera response was not considered, is due to the proportion of the dynamic range of the camera that was used; the camera function is better fit by a linear relationship when a smaller fraction of the dynamic range is used and, therefore, those cases with less excitation showed less error.

Apparent diffusion coefficient measurements for the three fluorescently labeled proteins are shown in Fig. 5. Three of the data sets were analyzed without taking into account the camera response function; they show accurate measurements only at the faster flow rates. Measurements of both streptavidin and ovalbumin reached maximal convergence with literature values by a flow rate of 500 nl/s, whereas measurements of insulin stabilized by 1 μl/s. An additional data set for ovalbumin was analyzed using the camera response curve and, as in the fluorescein-biotin case, accurate measurements were achieved even at low flow rates. All data indicate that if the camera response curve is taken into account, accurate diffusion measurements are possible with this device for molecules as large as proteins at all flow rates.

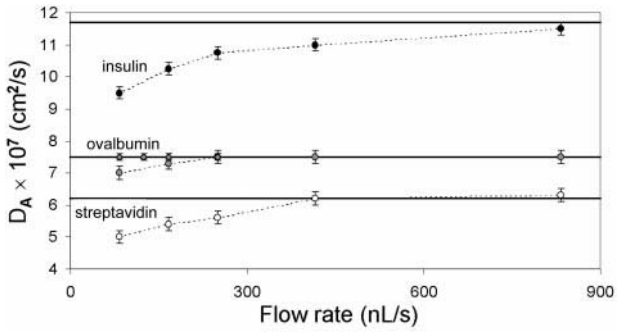

FIGURE 5 Apparent diffusion coefficient measurements for three fluorescently labeled proteins. Experiments were conducted at full excitation intensity. All data sets shown as circles were processed without taking into account the camera response function; the data set for ovalbumin (*diamonds*) was corrected for the camera response. The solid lines represent values for the diffusion coefficient obtained from literature: 11.0×10^{-7} cm^2/s for insulin (Walters et al., 1984), 7.5×10^{-7} cm^2/s for ovalbumin (Liu et al., 1993), and 6.2×10^{-7} cm^2/s for streptavidin (Perry, 1950), based on reported measurements of molecules of similar mass. The results are the same as for fluorescein-biotin; failure to consider the camera response function gives accurate measurements only at high flow rates, whereas consideration of the camera response allows accurate measurements over the entire flow rate range.

Quantification of entry effects

The three-dimensional hydrodynamic simulations of the 10-μm-wide T-sensor predicted an entry length for flow development. The predictions were made based on the value of the velocity along the center-centerline, that is at ½ *d* and ½ *w* (dotted line in Fig. 2 *A*), starting at the stagnation point where the two input legs merge. For three total flow rates of 41.67, 500, and 1000 nl/s, the distance to 95% of fully developed flow was 863.7 $\pm$ 1.5 μm, whereas that to 99% of fully developed flow was 1423 $\pm$ 5 μm. The small standard deviations indicate that entry length is independent of flow rate in the range studied.

Many aspects of the flow in a T-sensor with such a high aspect ratio can be treated as if the geometry is analogous to flow between infinite parallel plates (White, 1994). Most notably, the effective hydrodynamic length parameter used in many calculations reduces to the value of *w*. However, the values for entry length predicted by the three-dimensional model are not consistent with predictions of traditional fluid mechanics rules of thumb. This is due to the influence of the velocity profiles within the inlet legs on the development of the velocity along the main channel centerline. Therefore, the entry length should be dependent also on the size of the *d*-dimension and the geometry of the merge between the input legs.

The one-dimensional model used in this study does not consider flow development but rather assumes fully developed flow at all positions in the channel. Therefore, the model underpredicts the residence time for molecules traveling on the centerline, because the actual elapsed time for that fluid is greater due to the slower velocity in the development region. This error can be quantified by comparing the residence time for a hypothetical non-diffusing particle traveling along the center-centerline in the simplified one-dimensional model and the realistic three-dimensional simulations. At a distance of 5000 μm downstream, the one-dimensional model underpredicts the residence time for the three flow rates by 29.0 $\pm$ 2.2%, which results in an overprediction of the diffusion coefficient by the same percentage. This represents the worst-case scenario, because for any diffusable analyte, the actual error is much less since the fluid velocities adjacent to the centerline develop much more quickly. At a distance across *d* of 100 μm from the centerline, the residence time underprediction falls to 9%, and at 175 μm, it is only 4%. Since the analytes used in practice undergo substantial diffusion across the *d*-dimension, the estimated error from entry effects is less than 5%.

CONCLUSIONS

This work presented the T-sensor as a tool for measuring the diffusion coefficient of proteins and small molecules. Because it is very fast (image integration times $\leq$7 s), it may be preferable to other methods of measuring the diffusion

coefficient. The relatively small sample volumes (<10 μl) and amount of material (25–500 pmol) are not prohibitive for most applications. In addition, this method of measurement is insensitive to any nonfluorescent components of the sample, eliminating the need for a homogeneous sample required by methods such as dynamic light scattering (Schurr, 1977).

Diffusion coefficients were successfully measured for molecules ranging in mass from ~800 D to ~66 kD. In addition, an accurate measurement of diffusion coefficient for an even smaller molecule, albumin blue 580, with a mass of just 307 Daltons was made in a previous T-sensor study (Kamholz et al., 1999). The value of 4.6×10^{-6} cm^2/s for albumin blue (note the error in exponent in the source paper) is consistent with determinations made for sugars with similar masses. Thus, T-sensor accuracy for this type of measurement has been demonstrated over two orders of magnitude of molecular mass.

The importance of calibration of the camera response should be emphasized. Although neglecting this relationship allowed accurate measurements at higher flow rates, the method is applicable to the entire flow rate range only when the camera response is included in the analysis. Fortunately, calibration of the camera system response is relatively simple.

As discussed earlier, a key design feature of the microfluidic system described is that the T-sensor had a width (and, therefore, an optical path) of just 10 μm. This avoided complications from position-dependent downstream velocities, a situation that has been modeled for devices with larger widths (Kamholz and Yager, 2001). The demonstration of accurate diffusion coefficient measurements for both small molecules and macromolecules lays the groundwork for design of quantitative microfluidic assays involving diffusion perpendicular to the direction of flow.

This work was supported by DARPA MicroFlumes contract N660001–97-C-8632. The authors thank Mr. H. Sho Fuji and Mr. Gary Holman of the Washington Technology Center, Dr. Bernhard Weigl and the team at Micronics, Inc. (Redmond, WA), and Dr. John Harley of Microcosm, Inc. (Cary, NC). Most importantly, the authors acknowledge the continual support of the members of the Yager research group, particularly Ms. Catherine Cabrera, Mr. Anson Hatch, Mr. Kenneth Hawkins, Mr. Matthew Munson, Dr. Shelli Dennis, and Dr. Katerina Macounova, for essential scientific discussions and Ms. Cabrera for providing custom code for image analysis.

REFERENCES

Bernard, A., E. Delamarche, H. Schmid, B. Michel, H. R. Bosshard, and H. Biebuyck. 1998. Printing patterns of proteins. *Langmuir.* 14:2225–2229.

Brody, J. P., A. E. Kamholz, and P. Yager. 1997. Prominent microscopic effects in microfabricated fluidic analysis systems. *In* Proceedings of Micro- and Nanofabricated Electro-Optical Mechanical Systems for Biomedical and Environmental Applications. 103–110.

Chan, J. H., A. T. Timperman, D. Qin, and R. Aebersold. 1999. Microfabricated polymer devices for automated sample delivery of peptides for analysis by electrospray ionization tandem mass spectrometry. *Anal. Chem.* 71:4437–4444.

Chen, Y. H., and S. H. Chen. 2000. Analysis of DNA fragments by microchip electrophoresis fabricated on poly(methyl methacrylate) substrates using a wire-imprinting method. *Electrophoresis.* 21:165–170.

Chiu, D. T., N. L. Jeon, S. Huang, R. S. Kane, C. J. Wargo, I. S. Choi, D. E. Ingber, and G. M. Whitesides. 2000. Patterned deposition of cells and proteins onto surfaces by using three-dimensional microfluidic systems. *Proc. Natl. Acad. Sci. USA.* 97:2408–2413.

Crank, J. 1956. The Mathematics of Diffusion. Clarendon Press, Oxford. 347 pp.

Ehrlich, D. J., and P. Matsudaira. 1999. Microfluidic devices for DNA analysis. *Trends Biotechnol.* 17:315–319.

Folch, A., and M. Toner. 1998. Cellular micropatterns on biocompatible materials. *Biotechnol. Prog.* 14:388–392.

Galambos, P., F. K. Forster, and B. H. Weigl. 1997. A method for determination of pH using a T-sensor. *Transducers 97, Category 5-Chemical Sensors*.

Happel, J., and H. Brenner. 1973. Low Reynolds Number Hydrodynamics. Noordhoff International Publishing, Leiden, The Netherlands. 569 pp.

Kamholz, A. E., B. H. Weigl, B. A. Finlayson, and P. Yager. 1999. Quantitative analysis of molecular interaction in a microfluidic channel: the T-sensor. *Anal. Chem.* 71:5340–5347.

Kamholz, A. E., and P. Yager. 2001. Theoretical analysis of molecular diffusion in pressure-driven flow in microfluidic channels. *Biophys. J.* 80:155–160.

Kenis, P. J., R. F. Ismagilov, and G. M. Whitesides. 1999. Microfabrication inside capillaries using multiphase laminar flow patterning. *Science.* 285:83–85.

Khandurina, J., T. E. McKnight, S. C. Jacobson, L. C. Waters, R. S. Foote, and J. M. Ramsey. 2000. Integrated system for rapid PCR-based DNA analysis in microfluidic devices. *Anal. Chem.* 72:2995–3000.

Li, J., J. F. Kelly, I. Chernushevich, D. J. Harrison, and P. Thibault. 2000. Separation and identification of peptides from gel-isolated membrane proteins using a microfabricated device for combined capillary electrophoresis/nanoelectrospray mass spectrometry. *Anal. Chem.* 72: 599–609.

Liu, M. K., P. Li, and J. C. Giddings. 1993. Rapid protein separation and diffusion coefficient measurement by frit inlet flow field-flow fractionation. *Protein Sci.* 2:1520–1531.

Macounova, K., C. R. Cabrera, M. R. Holl, and P. Yager. 2000. Generation of natural pH gradients in microfluidic channels for use in isoelectric focusing. *Anal. Chem.* 72:3745–3751.

Perry, J. H., ed. 1950. Chemical Engineer's Handbook. McGraw-Hill, New York. 2609 pp.

Pinto, D. M., Y. Ning, and D. Figeys. 2000. An enhanced microfluidic chip coupled to an electrospray Qstar mass spectrometer for protein identification. *Electrophoresis.* 21:181–190.

Schurr, J. M. 1977. Dynamic light scattering of biopolymers and biocolloids. *CRC Crit. Rev. Biochem.* 4:371–431.

Walters, R. R., J. F. Graham, R. M. Moore, and D. J. Anderson. 1984. Protein diffusion coefficient measurements by laminar flow analysis: method and applications. *Anal. Biochem.* 140:190–195.

Weigl, B., and P. Yager. 1999. Microfluidic diffusion-based separation and detection. *Science.* 283:346–347.

White, F. M. 1994. Fluid Mechanics. McGraw-Hill, New York. 736 pp.

Yang, J., Y. Huang, X. B. Wang, F. F. Becker, and P. R. C. Gascoyne. 2000. Differential analysis of human leukocytes by dielectrophoretic field-flow-fractionation. *Biophys. J.* 78:2680–2689.